eISSN 2005-5447
International Journal of Stem Cells Vol. 16, No. 2, 2023 https://doi.org/10.15283/ijsc23001

ORIGINAL ARTICLE

Cyclic Phytosphingosine-1-Phosphate Primed Mesenchymal Stem Cells Ameliorate LPS-Induced Acute Lung Injury in Mice

Youngheon Park[1,*], Jimin Jang[1,*], Jooyeon Lee[1], Hyosin Baek[1], Jaehyun Park[1], Sang-Ryul Cha[1], Se Bi Lee[1], Sunghun Na[2], Jae-Woo Kwon[3], Seok-Ho Hong[3], Se-Ran Yang[1]

[1]*Department of Thoracic and Cardiovascular Surgery, School of Medicine, Kangwon National University, Chuncheon, Korea*
[2]*Department of Obstetrics and Gynecology, School of Medicine, Kangwon National University, Chuncheon, Korea*
[3]*Department of Internal Medicine, School of Medicine, Kangwon National University, Chuncheon, Korea*

Background and Objectives: O-cyclic phytosphingosine-1-phosphate (cP1P) is a synthetic chemical and has a structure like sphingosine-1-phosphate (S1P). S1P is known to promote cell migration, invasion, proliferation, and anti-apoptosis through hippocampal signals. However, S1P mediated cellular-, molecular mechanism is still remained in the lung. Acute lung injury (ALI) and its severe form acute respiratory distress syndrome (ARDS) are characterized by excessive immune response, increased vascular permeability, alveolar-peritoneal barrier collapse, and edema. In this study, we determined whether cP1P primed human dermal derived mesenchymal stem cells (hdMSCs) ameliorate lung injury and its therapeutic pathway in ALI mice.

Methods and Results: cP1P treatment significantly stimulated MSC migration and invasion ability. In cytokine array, secretion of vascular-related factors was increased in cP1P primed hdMSCs ($hdMSC^{cP1P}$), and cP1P treatment induced inhibition of Lats while increased phosphorylation of Yap. We next determined whether $hdMSC^{cP1P}$ reduce inflammatory response in LPS exposed mice. $hdMSC^{cP1P}$ further decreased infiltration of macrophage and neutrophil, and release of TNF-α, IL-1β, and IL-6 were reduced rather than naïve hdMSC treatment. In addition, phosphorylation of STAT1 and expression of iNOS were significantly decreased in the lungs of MSC^{cP1P} treated mice.

Conclusions: Taken together, these data suggest that cP1P treatment enhances hdMSC migration in regulation of Hippo signaling and MSC^{cP1P} provide a therapeutic potential for ALI/ARDS treatment.

Keywords: cP1P, MSC, ALI, HIPPO, STAT1

Received: January 2, 2023, Revised: January 20, 2023, Accepted: February 6, 2023, Published online: April 30, 2023

Correspondence to **Seok-Ho Hong**
Department of Internal Medicine, School of Medicine, Kangwon National University, 1 Kangwondaehak-gil, Chuncheon 24341, Korea
Tel: +82-33-250-7819, Fax: +82-33-255-8809, E-mail: shhong@kangwon.ac.kr
Co-Correspondence to **Se-Ran Yang**
Department of Thoracic and Cardiovascular Surgery, School of Medicine, Kangwon National University, 1 Kangwondaehak-gil, Chuncheon 24341, Korea
Tel: +82-33-250-7883, Fax: +82-33-255-8809, E-mail: seran@kangwon.ac.kr
*These authors contributed equally to this work.

Introduction

Acute lung injury/acute respiratory distress syndrome (ALI/ARDS) are caused by bacteria and viruses, absorption, and severe chest trauma, and complications include pulmonary hypertension and failure of multiple organs (1). Characteristics of ALI/ARDS include lung structural abnormalities due to lung cell damage, excessive inflammation such as increased neutrophils, and edema due to increased pulmonary vascular permeability (2). The hospital mortality rate of ALI/ARDS is 30%～40%, accounting for 10% of all intensive care unit hospitalizations and 24% of patients with mechanical ventilation. Recently, various treatments such as antibiotic development apply with ALI/ARDS, however, it is still remained alternative treatments (3). Mesenchymal stem cells (MSCs) have been applied in various diseases such as acute kidney failure, myocardial infarction, type 1 diabetes, multiple sclerosis, and pulmonary fibrosis (4). After injury, MSCs move to injured site through cytokine gradient-related signals. Homed MSCs perform immune regulation, angiogenesis, anti-fibrotic, and anti-apoptotic functions (5). Therefore, the improvement of MSCs homing ability is directly associated with therapeutic effect in damaged tissues (6). Many researchers have conducted research focusing on priming to improve the therapeutic function of MSCs. MSCs priming approach mostly focuses on maximizing paracrine effect in injured tissues by activating defensive/protective cell mechanisms. It is known that various factors such as IL-1β, IL-17A, TNF-α, IFN-γ, IFN- α, TGF-β1, and LPS have been reported *in vivo* or *in vitro* (7).

Sphingosine-1-phosphate (S1P) is mainly secreted from platelets and is involved in cell migration, invasion, and proliferation (8). S1P has five receptors (S1PR1, S1PR2, S1PR3, S1PR4, and S1PR5) and binds to each receptor to transmit various cell signals (9). O-cyclic phytosphingosine-1-phosphate (cP1P) is an analogous compound of S1P and combines with the same receptors of S1P to perform similar functions. It has shown that treatment of cP1P improves glycolytic reprogramming and transplantation efficiency through mTOR-dependent HIF1α translation of MSCs (10). In preclinical experiments, MSCs secrete paracrine factors with immunomodulatory effect, and recently intravenous delivery MSCs in patients with ARDS is associated with a reduction in alveolar permeability protein which may reduce damage of lung endothelial- and epithelial cells (11). Here, in this study, we demonstrated that cP1P treatment increase hdMSCs migration, invasion ability, and further determined whether hdMSC^{cP1P} ameliorates acute lung injury in mice. These findings could provide therapeutic potential in the field of ALI/ARDS.

Materials and Methods

hdMSCs isolation and culture

The human skin sample was obtained after a cesarean section from the pregnant woman's abdomen at Kangwon National University Hospital. All procedures were approved by the Institutional Review Board of Kangwon National University Hospital (IRB 2016-10-005-002). In accordance with previous studies, hdMSCs isolation and expansion were performed (12). Skin samples were stored in 1% penicillin and streptomycin (P/S) (Thermo Fisher Scientific, MA, USA). and cold PBS and transported to the laboratory. The sample was washed several times with cold PBS, separated into 4～6 mm^2 sizes, and cultured with 1 mg/ml Dispase II (Sigma-Aldrich) at 4℃. After 24 hours, only epidermis is obtained from the seed tissue and the epidermis was sectioned to a size of 1 mm^2. It was explanted to 25～30 pieces per 100 mm^2 culture dish. FBS was treated on each piece and cultured at 37℃. After 4 hours, the plate was incubated with a DMEM/high glucose (Cytiva, Massachusetts, USA) to which 1% P/S and 10% FBS were added. Every day, it was observed until the cells moved from the seed tissue. A few days later, all tissues on the plate were removed when the cell confluence was 80 to 90%. The cells in the plate were extracted with 0.25% trypsin/EDTA (Thermo Fisher Scientific, MA, USA) and stored in liquid nitrogen to perform stock or subculture.

O-cyclic phytosphingosine-1-phosphate (cP1P) treatment

cP1P was obtained from AXCESO BIOPARMA (268, Haguiro, Dongan-gu, Anyang-si, Gyeonggi-do, Republic of Korea). cP1P was treated with 1 μM or 5 μM for 24 hours after 3 washes at 1×PBS after performing starvation on hdMSCs during overnight.

Scratch assay (migration assay)

hdMSCs were seeded at 1×10^5 in 6 well and cultured for 24 hours. After that,itwas washed three times with 1×PBS and starved for overnight in DMEM/high glucose and 1% P/S medium without FBS. The next day, each well was scratched to the same area using 1,000 μl tip and washed twice with PBS. Each well treated 0.5 to 5 μM cP1P with a medium and checked the scratched space at ×40 magnification. After 24 hours, well was washed twice with PBS, and methanol was treated for fixation, and the

scratched space was checked at ×40 magnification. The size of the gap according to time and throughput of cP1P was analyzed with Image J.

Invasion assay

Coating at 4℃ for 24 hours on an 8.0 μM pore trans well plate (SPL Hanging) with 200 to 300 g/ml Martrigel (Corning, New York, USA) 200 μl. After 24 hours, hdMSCs are seeded on the coated plate with or without 0.5～5 μM of cP1P. After 24 hours, each transwell was stained by CAMCO STAIN PAK solutions (Camco, Cambridge, USA).

Animals and experimental protocol

Prior to the follow-up, all animal procedures were approved by Kangwon National University's Institutional Animal Care and Use Committee (No. KW-180903-1) in accordance with the guidelines. C57BL/6 male mice, 7～8 weeks old, 20～23 g weight, and purchased from DooYeol Biotech. After restricting intake 4 hours before the experiment, 1 mg/kg of lipopolysaccharide (LPS) (L3755-100MG; Sigma-Aldrich) derived from E. coli O26:B6 was diluted in 50 μl of saline and injected intratracheal. After 4 hours, 5×10^5 hdMSCs were treated intravenously in mice and observed until the end of the experiment. The mouse anesthetized with 10% zoletil (Virbac Corp., Fort Worth, TX, USA) after 24 hours LPS treatment and sacrificed for analysis. Mice were weighed twice before and after LPS injection 24 hours.

Sample collection

The mice were sacrificed 24 hours after LPS was treated with intratracheal injection. The sacrificed mouse lung was separated and washed with PBS. For paraffin embedding, the left side tissue was fixed with 4% paraformaldehyde overnight. The opposite side tissue was homogenized several times for PCR and Western blot analysis and stored at −80℃.

Bronchoalveolar lavage fluid

An 18-gauge catheter was inserted into the bronchus to obtain Bronchoalveolar lavage fluid from the sacrificed mice, and then 1 ml of PBS was injected until the lungs swelled. After that, about 1ml of BALF was extracted by pulling the piston again. BALF was centrifuged at 3,000 rpm for 10 minutes to separate pellets. The supernatant was extracted in another 1.5 ml tube and stored at −80℃ and used in ELISA for cytokine measurement. The pellets were diluted with 1 ml of saline to proceed with Giemsa staining.

Transplantation of hdMSCs

Confirmation of hdMSCs injection by expression of chromosome 17. mRNA was extracted using Trizol and chloroform from lung tissue obtained from sacrificed mice injected with hdMSCs. mRNA was synthesized into cDNA by a reverse transcription kit (EBT-1514) (ELPIS-BIOTECH, Daejeon, Republic of Korea). cDNA was synthesized into chromosome 17 by PCR premix kit and then loaded into 5% agarose gel. The PCR band was analyzed as Bioprint CX4 (Bio-Rad, CA, USA).

Lung tissue histology

Obtain 4% formaldehyde-treated lung tissue for 24 hours and commission to a histologist for paraffin blocks and slides. The tissue part was sectioned with a thickness of 4 μM, and then H&E stains were performed. The slide was analyzed at ×100 magnification to evaluate as describe elsewhere (13). In brief, lung injury score was based on five parameters: neutrophils in the alveolar space, neutrophils in the interstitial space, hyaline membranes, proteinaceous debris filling the airspaces, and alveolar septal thickening with blind test. Each parameter has a different distribution point, and each scores are combined.

Enzyme-linked immunosorbent assay (ELISA)

The obtained lung tissue was stored at −80℃ for 24 hours and homogenized. After treating the 1 ml RIPA dissolution buffer solution, vortexing was performed three times every 10 minutes and centrifuged to 13,000 G, 10 minutes to obtain a supernatant. The supernatant and BALF supernatant quantified by BCA analysis were measured IL-6, TNF-α, and IL-1β using the ELISA kit (DY406, DY410, DY401) (R&D systems, Minneapolis, USA). In brief, 96 microplates were treated with capture antibody at room temperature for overnight. Next day the plate was washed with PBS with 0.05% tween 20, and then blocking buffer was treated for 1 hour and washed twice. Thereafter, lung homogeneous, BALF samples and standard were treated. Two hours later, detection antibody was treated for 2 hours, washed twice, and streptavidin Horseradish Peroxidase (HRP) was treated for 20 minutes at room temperature. After washing threetimes, color reagent A (H_2O_2) and B (tetramethylbenzidine) were mixed 1 : 1 and treated at room temperature for 20 minutes. Finally, H_2SO_4 was treated to suppress the reaction. When the color changed to yellow, it was measured with an absorbance of 450 nm.

Giemsa staining

Pellets obtained from centrifuged BALF were diluted with 1 ml saline. Cytocentrifuge was performed on a

poly-L-Lysine coated slide at ×3,000 G, 10 minutes. The slide was stained with a CAMCO STAIN PAK kit (Camco, Cambridge, USA). It consists of three solutions of kits. In a nutshell, solution1 was treated on the slide for 1 minute to fix the cells. After washing, solution2 for dyeing cytoplasm was treated. Finally, solution3 to dye the nucleus was treated and washed with distilled water. We analyzed the neutrophils, macrophages, and total number of cells with images obtained using microscope. The images were captured at ×200 magnification.

Real-time quantitative PCR

Lung tissue obtained from mice was treated with Trizol (Ambion, Texas, USA) and chloroform after homogenization. After centrifugation at 13,000 rpm and 4℃ for 15 minutes, only the supernatant was obtained, and isopropanol was treated. After centrifugation at 13,000 rpm and 4℃ for 15 minutes, the supernatant was discarded and washed with 70% EtOH. The pellet was dried and treated with RNase free water. In the case of real-time quantitative PCR, the total mRNA was quantified to 1 μg and cDNA was synthesized using Reverse Transcription Master Premix. The expression of target gene was compared relatively using two housekeeping genes, β-actin and glyceraldehyde 3-phosphate dehydrogenase (GAPDH). Gene expression in qPCR devices was calculated as $2^{-\Delta\Delta CT}$. Primers for target genes are listed in Table 1.

Western blot analysis

Lung tissue obtained from mice was treated with RIPA cocktails (50 nM Tris-HCL, pH 7.5, 15 M NaCl, 1% Triton-X-100, 1% sodium deoxycholate, 0.1% SDS) and repeatedly vortexed and stored at −80℃. After one day, the mixture was centrifuged at 14,000 G to obtain only supernatant, and the total protein in the sample was measured through BCA analysis. Western blot samples were pre-

Table 1. Sequences of the primers in PCR analysis

Gene	5′-3′ sequence	Accession number
Chromosome 17-α satellite	F: GGGATAATTTCAGCTGACTAAACAG R: TTCCGTTTAGTTAGGTGCAGTTATC	NC_000017.11
Real-time PCR		
MMP2	F: CCCCCAAAACGGACAAA R: GCAGCCATAGAAGGTGTTCA	NM_004530.6
MMP9	F: GCCCCGGCATTCAG R: AGGGACCACAACTCGTCAT	NM_004994.3
S1PR1	F: CTCCCGCCCAGTGGTT R: TGACAGGGCCACAAACATA	NM_001400.5
S1PR2	F: GCCCGAAACAGCAAGTTC R: CCAGGTTGCCCAGAAAC	NM_004230.4
S1PR3	F: TCGACCCAAGCAGAAGTAAA R: TTCGGAGAGTGGCTGCTA	NM_005226.4
S1PR4	F: TGCCTGTGCGCCTTT R: GATGTAGCGCTTGGAGTAGAG	NM_003775.4
S1PR5	F: CCATGGCCAACTCACTTCTG R: GCAGGTCGCGGTTGGT	NM_030760.5
YAP1	F: GAGGCTGCGGCTGAAAC R: GGATTGATATTCCGCATTGC	NM_001130145.3
TAZ	F: CACCTGACCGTGCACAA R: GCCTCGCTTCTCGATGAG	NM_000116.5
TEAD1	F: AAGACGTCAAGCCTTTTGTG R: TGACCGCTGGCTGGAT	NM_021961.6
RHOA	F: GTTGGCTTTGTGGGACACA R: GGGCCTCAGGCGATCA	NM_001664.4
SLUG	F: GCTACCCAATGGCCTCTCT R: CACTCGCCCCAAAGATG	NM_003068.5
CTGF	F: ACCTGTGGGATGGGCATCT R: CCTGCAGGAGGCGTTGT	NM_001901.3
AREG	F: GGTGCTGTCGCTCTTGATA R: GGTCCAATCCAGCAGCAT	NM_001657.4

pared by mixing 25 μg totalprotein, a 5× loading buffer, and D.W. The sample was heated for 7 minutes and 100℃. Depending on the protein size, the sample was run in an 8%～15% SDS-PAGE gel for 2 hours, and then a 0.45 μM nitrocellulose transfer membrane was placed on the gel and transferred to the membrane with 100 V for 15 hours. After transfer, the membrane was stained by Ponceau S to confirm the protein band and washed with 1×TBST (tris buffered saline 0.05% Tween 20). After washing, it was blocked with 5% skim milk for 1 hour and washed with 1×TBST. The first antibody: anti-Inos (sc-650) (Santa Cruz Biotechnology, CA, USA), anti-pLats1 (Thr1079) (#8654), anti-Lats1 (#3477), anti-pYap (Ser 127) (#13008), anti-Yap, anti-pSTAT1 (Ser727) (#9177), anti-STAT1 (#9172), anti-β-actin (#3700) (Cell Signaling Technology, MA, USA) diluted at 1 : 1,000～10,000 was treated for 4 hoursand washed again. The secondary antibody was treated for 1 hour and washed. After ECL was treated on the membrane, a band was identified by Chemi Doc. Using β-actin and GAPDH, the sizes of each band were fold-changed and compared.

Human cytokine antibody array

hdMSCs were seeded by 1×10^6 on a 150 mm dish with a DMEM/high glucose medium and cultured for 24 hours. Each plate starved overnight with a non-FBS medium and then treated cP1P. After 24 hours, 2 ml of supernatant was collected for each plate and centrifuged at 3,000 rpm. The paracrine factor was detected with a human cytokine array kit (ARY022B, R&D systems, MN, USA) according to the manufacturer protocol. After the experiment, the array membrane was snapped by Chemi Doc (BIO-RAD, CA, USA) and analyzed with image lab software.

Statistical analysis

All *in vitro* and *in vivo* experiments were performed at least 3 times. Each result was performed by GraphPad Prism 9 software (GraphPad Software, CA, USA). Comparison of parameters between 2 groups was made by Student's t-test. Comparison of parameters in more than 2 groups was tested through one-way analysis of variance and followed by Bonferroni *post hoc* test for repeated measurement tests. The p-value calculated for statistical significance was expressed as $^*p<0.05$, $^{**}p<0.01$, and $^{***}p<0.001$.

Results

hdMSCs treated with cP1P were promoted homing by enhanced migration and invasion

cP1P is an analog compound of S1P, it forms a cyclic structure at the end to be more stable than S1P (Fig. 1A). In order to determine cytotoxicity of cP1P in hdMSCs, hdMSCs were treated with cP1P at a concentration of 0.5～5 μM for 24 hours. As shown Fig. 1B, treatment of cP1P did not affect cell viability of hdMSCs in the range of 0.5～5 μM. We next evaluated hdMSC migration capacity by introducing scratch test to assess wound area. hdMSCs were seeded by 5×10^4 and incubated, then cP1P was treated in hdMSCs for 24 hours. hdMSC migration significantly increased at concentration of cP1P 0.5 μM and 1 μM, and slightly decreased at 5 μM of cP1P (Fig. 2A and 2B). Accordingly, we conducted transwell migration assay and crystal violet staining to determine migrated MSCs. In migration assay, invasion was significantly increased at 1 μM and 5 μM cP1P (Fig. 2C), moreover, mRNA levels of MMP2 and MMP9, which are associated with invasion factors, were increased in RT-PCR analysis (Fig. 2D). These data suggest that cP1P improves migration and invasion capabilities of hdMSCs.

cP1P increases secretome of hdMSC in regulation of hippo signaling of hdMSC

To investigate whether cP1P affects the cytokine secretion profile of hdMSCs, cytokine array was carried out in the supernatant of hdMSC. In cytokine array, the presence and relative amount of 105 cytokines were analyzed. Notably, increases of in the expression of VEGF, ICAM-1, CHI3L1, CD31, DKK1 were observed, and a number of increased cytokines were associated with angiogenesis and tissue repair-related factors (Fig. 3A). Activation of Hippo signaling pathway is essential for a wide range of cellular processes including cell proliferation, migration and tissue repair. Therefore, we next determined whether cP1P primed MSCs is associated with underlying signaling of Hippo pathway. Firstly, mRNA levels of the five S1PR subtypes including S1PR1, S1PR2, S1PR3, S1PR4, S1PR5 were determined by RT-PCR analysis. As shown in Fig. 3C, cP1P treatment upregulated mRNA levels of in the five S1PR1 to 5 subtypes. Accordingly, we determined mRNA expression of RHOA, YAP, TAZ, TEAD, CTGF, AREG, and SLUG, which are associated with Hippo signal pathway were remarkably increased (Fig. 3C). In addition, cP1P primed MSCs exhibited increased phosphorylation of Yap while decreased phosphorylation of Lats1 in western blot analysis (Fig. 3D). These results demonstrate that cP1P

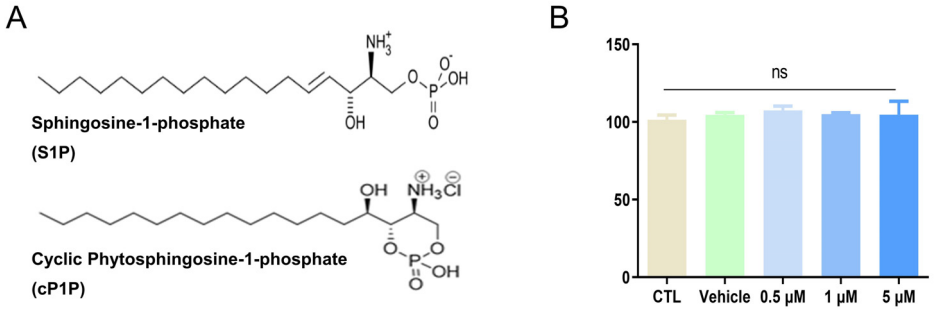

Fig. 1. An analogous compound of S1P, cP1P does not have cellular toxicity. (A) Structural formula of S1P and cP1P. (B) Cell viability was quantified by MTT assay at various concentrations (Vehicle, 0.5, 1, 5 μM). All data are representative of multiple experiments. CTL: control group, ns: not significant.

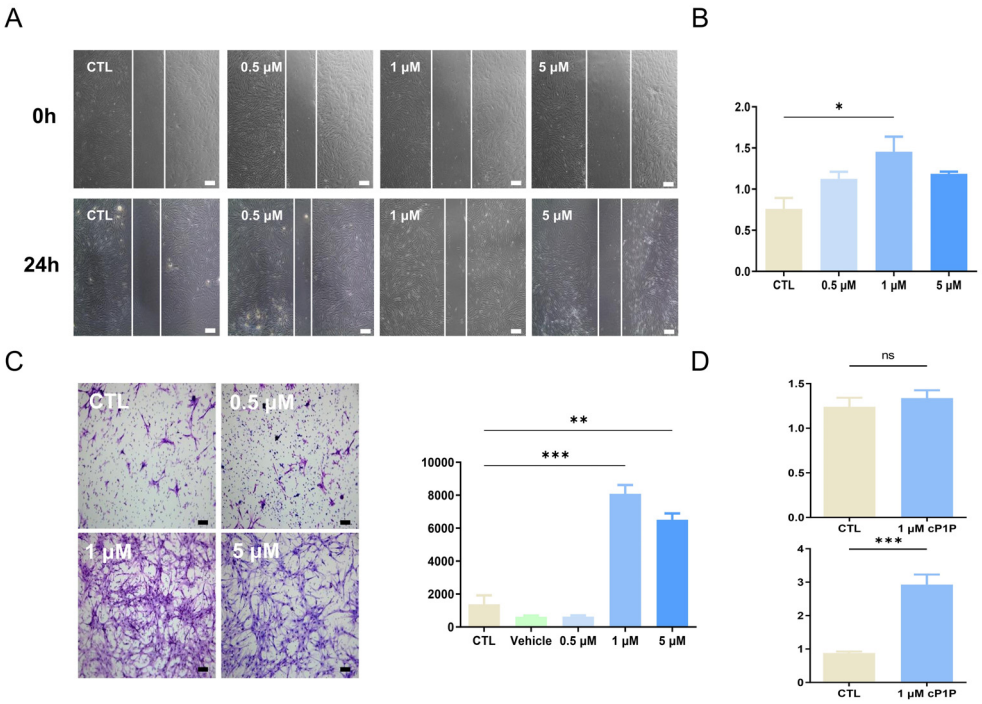

Fig. 2. hdMSC^{cP1P} was promoted homing by upregulated migration and invasion. (A) hdMSCs scratched by 1 ml tips and then treated to cP1P (0.5 μM, 1 μM, 5 μM) for 24 h. Scratch point captured by microscope (magnification ×40, Scale bars, 100 μm). (B) Wound healing degree of MSC was quantified by migration assay. After 24 h, various concentration was measured and presented as fold change. (C) Invasion assay was measured by trans well. Various concentrations. Original magnification, ×40. Scale bars, 100 μm. Cell numbers of various concentrations was counted and presented as numbers. (D) gene expression level of MMP2 and MMP9 was measured by real-time PCR. All data are representative of multiple experiments. CTL: control group, ns: not significant. *p<0.05, **p<0.01, and ***p<0.001 vs. control group.

priming stimulates secretome of hdMSC, and it is associated with Lats-Yap/Taz signaling pathway.

cP1P primed hdMSCs ameliorate lung injury in LPS induced ALI mice

We next determined whether cP1P primed hdMSCs (hdMSCs^{cP1P}) attenuate alveolar injury. hdMSCs or hdMSCs^{cP1P} intravenously administered at 4 hours after LPS exposure. After 24 hours, mice were killed, and lungs were harvested. Histology of lungs were evaluated by measuring the mean alveolar size, alveolar wall thickness and the lung injury system by Matute-Bello's procedure as markers of lung injury. In the lungs of mouse, lung injury scores were quantified using a parameter 0, 1, 2, and calculated. In H&E staining, LPS treated with hdMSC^{cP1P} group showed significant lower lung injury score compared to the LPS alone group and LPS with hdMSCs group (Fig. 4A and 4B). As a result of measurement weight ratio of mice before and after LPS treatment, there was no significant difference between the LPS treatment group and the LPS with hdMSC^{cP1P} group (Fig. 4C). However, when mouse lung weight per body weight was measured, the ra-

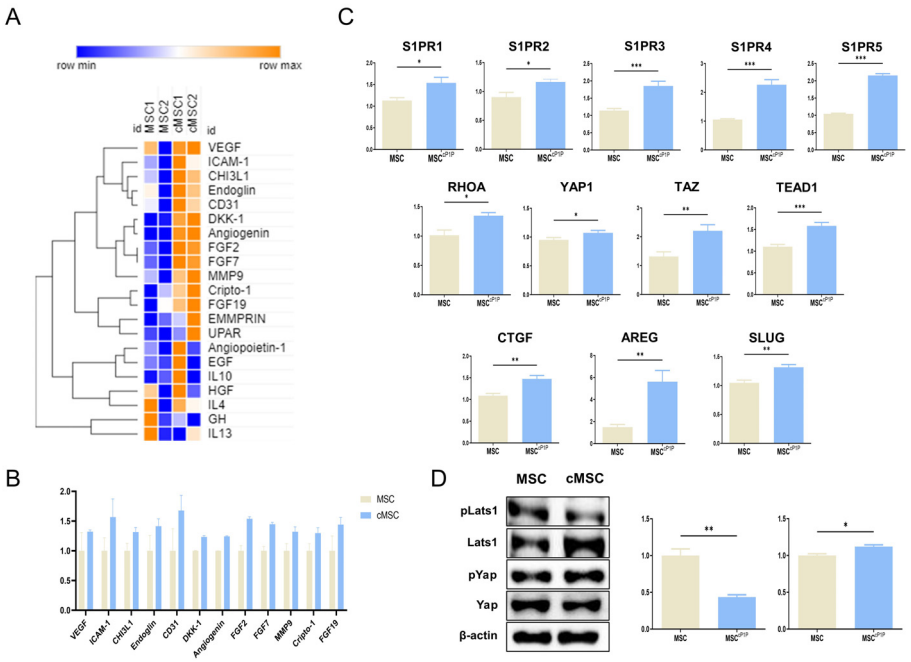

Fig. 3. Changes in cytokines secreted by cP1P in hdMSC. (A) Heat map of hdMSC^{cP1P} and non-primed hdMSC. Changes of cytokines were measured by cytokine assay kits. (B) Comparison of mean pixel density measurement between hdMSC and cP1P-primed hdMSC. (C) 1 μM cP1P-primed hdMSC and non-primed hdMSC measured mRNA expression level of hippo signaling pathway and migration associated factors by Real-time PCR. (D) Protein level of Lats1, YAP1 measured by Western blot. All data are representative of multiple experiments. CTL: control group, MSC^{cP1P}: 1 μM cP1P-primed hdMSC, ns: not significant. *p<0.05, **p<0.01, and ***p<0.001 vs. MSC group.

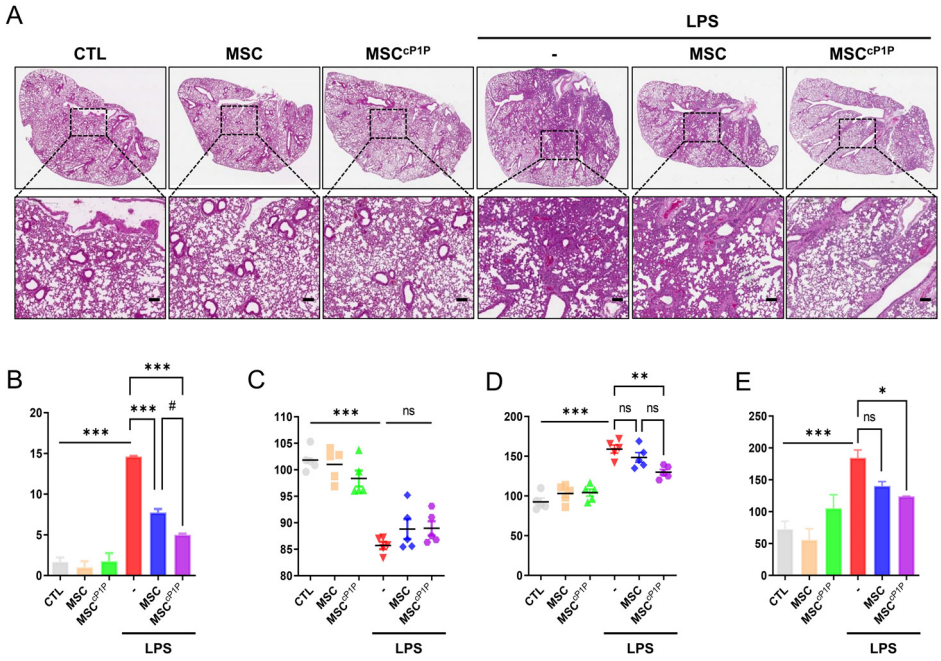

Fig. 4. hdMSC^{cP1P} ameliorates LPS-induced acute lung injury. (A) Histopathological examinations of lung tissue. Mouse lung sections were stained by H&E staining. Original magnification, ×100. Scale bars, 200 μm. (B) Bar graphs showing blinded analysis of lung injury score. (C) Mouse weight before and after treating LPS was measured in each group. (D) Mouse lung weight per body weight was measured in each group. (E) Total protein in BALF was quantified by BCA assay. All data are representative of multiple experiments. CTL: control group, MSC^{cP1P}: 1 μM cP1P-primed hdMSC, ns: not significant. *p<0.05, **p<0.01, and ***p<0.001 vs. LPS groups; $^{\#}$p<0.05 vs. LPS treated MSC^{cP1P} groups.

tio was increased in LPS group, while the ratio significantly decreased in hdMSC^{cP1P} group (Fig. 4D). In consistent with lung injury score, total protein concentration in BALF obtained BCA assay tended to decrease in hdMSC^{cP1P} group compared to LPS alone and LPS with hdMSCs group (Fig. 4E).

hdMSCscP1P ameliorates alveolar inflammation through STAT1/iNOS pathway in ALI mice

Excessive inflammation or disruption of vascular permeability is associated with pathogenesis of ALI/ARDS. Therefore, we next determined whether hdMSCs^{cP1P} alleviate alveolar inflammation and its associated pathological pathway. In our previous data, we have shown that hdMSCs^{cP1P} possess ability to alleviate tissue injury through higher migration and invasion function compared to non-primed hdMSCs. In addition, Giemsa stain and ELISA were performed to confirm whether cP1P primed hdMSCs adjusted the immune response in mice after LPS exposure. Macrophages and neutrophils in BALF of hdMSCs^{cP1P} engrafted mice were significantly decreased, and released cytokines including IL-6, TNF-α and IL-1β were reduced (Fig. 5A and 5B). The JAK-STAT signaling pathway has been associated with driving carcinogenesis and inflammation in the lung. In STAT members, STAT1 is a well-characterized factor that plays significant roles in many cellular process such as vascular formation as well as injury, and its activation by the interferons modulates immune responses. Therefore, we next determined whether engrafted hdMSCs^{cP1P} are associated with inhibition of phosphorylated STAT1 in ALI mice. Mice were intratracheally exposed to LPS and protein levels of STAT1 in the lung homogenates were determined in western blot analysis. As shown in Fig. 3C, LPS exposure increased phosphorylation of STAT1 while engrafted hdMSCs and hdMSCs^{cP1P} inhibited the phosphorylation of STAT1 in response to LPS injury. Moreover, expression of iNOS was increased in response to LPS, however hdMSCs and hdMSCs^{cP1P} treatment significantly reduced in ALI mice (Fig. 4C).

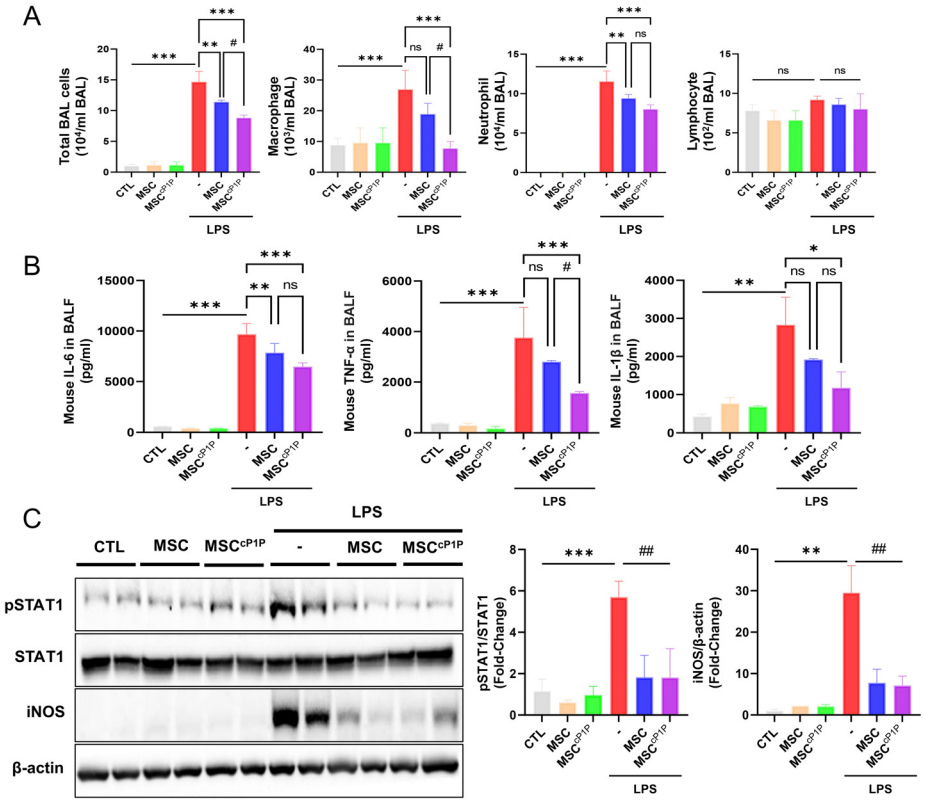

Fig. 5. hdMSC^{cP1P} ameliorates pro-inflammatory cytokine expression and inflammatory signaling pathway of LPS-induced acute lung injury. (A) Macrophages, neutrophils, lymphocytes, and total cells in BALF was counted at each groups. BALF cell was stained by Giemsa staining and counted each group. (B) Pro-inflammatory cytokines in BALF of each group was measured by ELISA. (C) inflammatory signaling factors of each group were quantified by western blot and expression ratio was measured as fold change. All data are representative of multiple experiments. CTL: control group, MSC^{cP1P}: 1 μM cP1P-primed hdMSC, ns: not significant. *p<0.05, **p<0.01, and ***p<0.001 vs. LPS groups; $^{\#}$p<0.05, $^{\#\#}$p<0.01 vs. LPS treated MSC^{cP1P} groups.

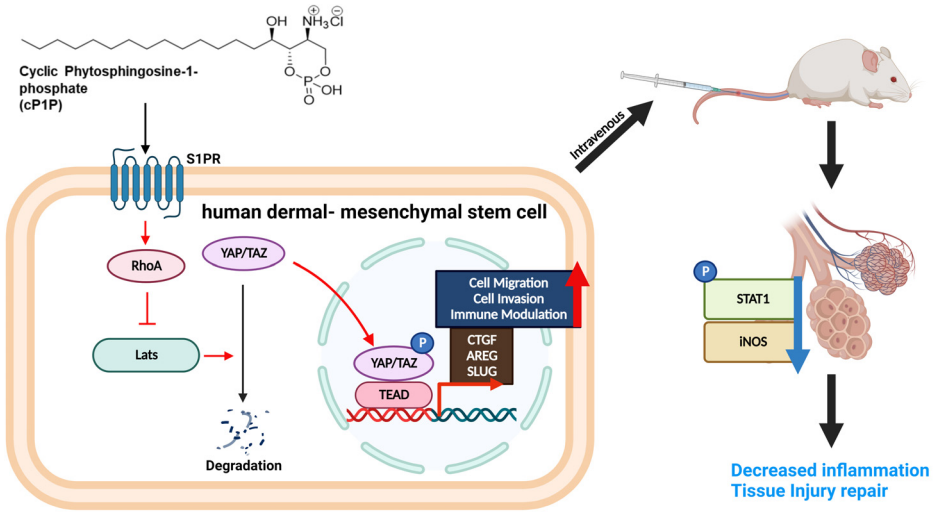

Fig. 6. cP1P acts as a ligand of the S1P receptor of hdMSCs, promoting Hippo signaling. Increased RhoA and reduced Lats1 cause nucleus-translocation of YAP/TAZ. YAP/TAZ acts as a transcription factor in TEAD gene site, increasing the expression of CTGF, AREG, and SLUG genes, enhancing the cell migration, invasion, and immune modulation functions of hdMSCs. Enhanced hdMSCs reduce p-STAT1 and iNOS, attenuating inflammation, and recovering damaged tissue LPS-induced ALI mice.

Discussion

Sphingosine-1-phosphate (S1P) is bioactive lysophospholipid that acts as an intracellular messenger. Although differential binding of receptor subtypes, cellular level of S1P regulates many pathological processes including obesity, insulin resistance, hyperglycemia, angiogenesis and caner (14, 15). S1P, as an extracellular ligand, mediated Hippo signaling by increasing expression of RHOA, YAP, and TAZ has been demonstrated in endothelial barrier function as well as the maintenance of vascular homeostasis (16). Hippo signaling consists of mammalian Sterile 20-related 1 and 2 kinases (MST1/2) and Large tumor suppressor 1 and 2 kinases (Lats1/2), Salvador1 (SAV1), MOB kinase activator 1A and 1B (MOB1A/B), the transcriptional co-activators YAP and TAZ, and TEA-domain containing sequence specific factors (TEAD1-4) (17). Our findings have shown that mRNA expression of S1PR was increased, moreover cP1P treatment led decreased expression of phosphorylated Lats while increased phosphorylation of YAP in hdMSCs. Particularly, phosphorylation of Lats is regarded as the last factor to in YAP from translating into nuclei in Hippo signaling (18, 19). In the progenitor cells of multiple tissues, activated level of YAP/TAZ has been observed. In contrast, inactivation of Hippo signaling has induced gene expression of CTGF, AREG, and SLUG, which affect the differentiation, proliferation, migration, and other biological functions of MSCs (20). Decrease of phosphorylated Lats plays an important role in improving the therapeutic function of hdMSCs by activating its function as a transcription factor of YAP.

Törnquist and Kalhori has reported that MMP2 and MMP9 which are facilitated proteolytic enzymes for degradation of the extracellular matrix participate in S1P-induced migration and invasion of both normal and cancer cells (21). In agreement with previous report, cP1P treatment significantly increased mRNA level of MMP9 leading to stimulate migration and invasion activity of hdMSCs. These findings suggest that cP1P via up-regulation of Hippo signaling improves homing ability of hdMSCs.

Since ALI/ARDS has been characterized by excessive inflammation, tissue damage, and increased risk of fibrosis after recovery (22), we investigated whether hdMSCs primed with cP1P inhibits alveolar inflammation and injury in ALI mice. It is well-known that the secretome including various cytokines and exosomes from MSCs facilitate therapeutic approach through homing effect (23).

We found that tissue repair or angiogenesis related secretory factors such as ICAM-1, DKK-1, Endoglin, and angiogenin were significantly increased in the cP1P priming hdMSCs. ICAM-1 is a factor involved in cell adhesion and affects immune response regulation and angiogenesis through increased MSCs homing (24, 25). In addition, DKK-1 is a Wnt β-catenin inhibitor that helps differentiation and tissue regeneration into AEC2 (26). Moreover, endoglin (CD105) is predominantly expressed in endothelial cells and it is contributed to induce vascular endothelial cells in repair of injured tissues and angiogenesis. Mao and colleagues reported that endoglin has been upregulated in the pulmonary microvasculature of ventilated preterm infants at risk for bronchopulmonary dysplasia (27). These results suggest that endoglin could be a potential candidate regulator of ventilation induced angiogenesis for development of bronchopulmonary dysplasia. In this study, our data suggest that hdMSC^{cP1P} enhance naïve MSCs and their abilityto release the upregulated secretary

cytokines of ICAM-1, DKK-1, Endoglin, and angiogenin in the injured microvasculature repair of ALI mice. Moreover, the wall thickness of alveoli and infiltration of immune cells by hdMSC^{cP1P} treatment were inhibited as well as immune regulation. These results are agreed with previous studies about effect of allogenic MSCs in LPS-induced ALI mice (28, 29). In addition, comparing the total protein concentration of BALF with the weight of the lungs, it has been confirmed that pulmonary edema, one of the characteristics of ARDS, is alleviated (30, 31). We have shown that hdMSC^{cP1P} treatment markedly reduced infiltration of macrophages as well as decreased pro-inflammatory cytokines including IL-6, IL-1β, and TNF-α in BALF. These suggest that enhanced hdMSCs is involved in blood vessel permeability as well as immunomodulatory function to prevent penetration of immune cells into the lungs. It has reported that NF-κB signaling pathway is responsible for treatment of LPS-induced ALI/ARDS (32). However, there was no significant difference between LPS and hdMSC treated groups (data not shown). On the other hand, hdMSC and hdMSC^{cP1P} administration were significantly decreased phosphorylation of STAT1 as well as increased protein level of iNOS in ALI mice. Macrophage NO is largely the product of iNOS, and preferentially induced iNOS in macrophages serve as a phenotypic marker of M1 macrophage (33). It has reported that STAT dimers translocated into the nucleusand bind to target gene,and specifically STAT1-iNOS signaling is involved in the secretion of pro-inflammatory cytokines (34). Therefore, our findings suggest that hdMSC^{cP1P} inhibitmacrophage infiltration through suppression of STAT1-iNOS signaling to alleviate inflammation. Our results demonstrate the enhanced role of hdMSC^{cP1P} in the treatment of acute lung injury, however it is necessary to determine repair mechanism of injury and vascular remodeling.

In conclusion, Taken together, our data suggest that hdMSC^{cP1P} possess higher homing capabilities into injuredareavia Hippo pathway, and further inhibit macrophage infiltration via STAT1/iNOS axis in ALI mice (Fig. 6). These findings contribute to understand cP1P mediated physiological signaling of MSCs, moreover, hdMSC^{cP1P} enhance therapeutic potential for ALI/ARDS and its related diseases.

Acknowledgments

This work was supported by the National Research Foundation (NRF) funded by the Korean government (MSIT) (2020R1A2C2010712, 2020R1A5A8019180), the Korean Fund for Regenerative Medicine (KFRM) (22A0304L1-01).

Potential Conflict of Interest

The authors have no conflicting financial interest.

References

1. Bakowitz M, Bruns B, McCunn M. Acute lung injury and the acute respiratory distress syndrome in the injured patient. Scand J Trauma Resusc Emerg Med 2012;20:54
2. Esper AM, Martin GS. Evolution of treatments for patients with acute lung injury. Expert Opin Investig Drugs 2005; 14:633-645
3. Sauer A, Peukert K, Putensen C, Bode C. Antibiotics as immunomodulators: a potential pharmacologic approach for ARDS treatment. Eur Respir Rev 2021;30:210093
4. Parekkadan B, Milwid JM. Mesenchymal stem cells as therapeutics. Annu Rev Biomed Eng 2010;12:87-117
5. Lin H, Xu R, Zhang Z, Chen L, Shi M, Wang FS. Implications of the immunoregulatory functions of mesenchymal stem cells in the treatment of human liver diseases. Cell Mol Immunol 2011;8:19-22
6. De Becker A, Riet IV. Homing and migration of mesenchymal stromal cells: how to improve the efficacy of cell therapy? World J Stem Cells 2016;8:73-87
7. Noronha NC, Mizukami A, Caliári-Oliveira C, Cominal JG, Rocha JLM, Covas DT, Swiech K, Malmegrim KCR. Priming approaches to improve the efficacy of mesenchymal stromal cell-based therapies. Stem Cell Res Ther 2019;10: 131 Erratum in: Stem Cell Res Ther 2019;10:132
8. English D, Welch Z, Kovala AT, Harvey K, Volpert OV, Brindley DN, Garcia JG. Sphingosine 1-phosphate released from platelets during clotting accounts for the potent endothelial cell chemotactic activity of blood serum and provides a novel link between hemostasis and angiogenesis. FASEB J 2000;14:2255-2265
9. Mendelson K, Evans T, Hla T. Sphingosine 1-phosphate signalling. Development 2014;141:5-9
10. Lee HJ, Jung YH, Choi GE, Kim JS, Chae CW, Lim JR, Kim SY, Lee JE, Park MC, Yoon JH, Choi MJ, Kim KS, Han HJ. O-cyclic phytosphingosine-1-phosphate stimulates HIF1α-dependent glycolytic reprogramming to enhance the therapeutic potential of mesenchymal stem cells. Cell Death Dis 2019;10:590
11. Wick KD, Leligdowicz A, Zhuo H, Ware LB, Matthay MA. Mesenchymal stromal cells reduce evidence of lung injury in patients with ARDS. JCI Insight 2021;6:e148983
12. Park JR, Kim E, Yang J, Lee H, Hong SH, Woo HM, Park SM, Na S, Yang SR. Isolation of human dermis derived mesenchymal stem cells using explants culture method: expansion and phenotypical characterization. Cell Tissue Bank 2015;16:209-218
13. Matute-Bello G, Downey G, Moore BB, Groshong SD, Matthay MA, Slutsky AS, Kuebler WM. An official American Thoracic Society workshop report: features and measurements of experimental acute lung injury in animals. Am J Respir Cell Mol Biol 2011;44:725-738
14. Xie Z, Liu H, Geng M. Targeting sphingosine-1-phosphate

signaling for cancer therapy. Sci China Life Sci 2017;60: 585-600
15. Kennedy S, Kane KA, Pyne NJ, Pyne S. Targeting sphingosine-1-phosphate signalling for cardioprotection. Curr Opin Pharmacol 2009;9:194-201
16. Mahajan-Thakur S, Bien-Möller S, Marx S, Schroeder H, Rauch BH. Sphingosine 1-phosphate (S1P) signaling in glioblastoma multiforme-a systematic review. Int J Mol Sci 2017;18:2448
17. Johnson R, Halder G. The two faces of Hippo: targeting the Hippo pathway for regenerative medicine and cancer treatment. Nat Rev Drug Discov 2014;13:63-79
18. Li L, Dong L, Wang Y, Zhang X, Yan J. Lats1/2-mediated alteration of Hippo signaling pathway regulates the fate of bone marrow-derived mesenchymal stem cells. Biomed Res Int 2018;2018:4387932
19. Li L, Dong L, Zhang J, Gao F, Hui J, Yan J. Mesenchymal stem cells with downregulated Hippo signaling attenuate lung injury in mice with lipopolysaccharide-induced acute respiratory distress syndrome. Int J Mol Med 2019;43:1241-1252
20. Yu FX, Zhao B, Guan KL. Hippo pathway in organ size control, tissue homeostasis, and cancer. Cell 2015;163:811-828
21. Kalhori V, Törnquist K. MMP2 and MMP9 participate in S1P-induced invasion of follicular ML-1 thyroid cancer cells. Mol Cell Endocrinol 2015;404:113-122
22. Burnham EL, Janssen WJ, Riches DW, Moss M, Downey GP. The fibroproliferative response in acute respiratory distress syndrome: mechanisms and clinical significance. Eur Respir J 2014;43:276-285
23. Willis GR, Fernandez-Gonzalez A, Anastas J, Vitali SH, Liu X, Ericsson M, Kwong A, Mitsialis SA, Kourembanas S. Mesenchymal stromal cell exosomes ameliorate experimental bronchopulmonary dysplasia and restore lung function through macrophage immunomodulation. Am J Respir Crit Care Med 2018;197:104-116
24. Gho YS, Kleinman HK, Sosne G. Angiogenic activity of human soluble intercellular adhesion molecule-1. Cancer Res 1999;59:5128-5132
25. Tang B, Li X, Liu Y, Chen X, Li X, Chu Y, Zhu H, Liu W, Xu F, Zhou F, Zhang Y. The therapeutic effect of ICAM-1-overexpressing mesenchymal stem cells on acute graft-versus-host disease. Cell Physiol Biochem 2018;46: 2624-2635
26. Sun Z, Gong X, Zhu H, Wang C, Xu X, Cui D, Qian W, Han X. Inhibition of Wnt/β-catenin signaling promotes engraftment of mesenchymal stem cells to repair lung injury. J Cell Physiol 2014;229:213-224
27. De Paepe ME, Patel C, Tsai A, Gundavarapu S, Mao Q. Endoglin (CD105) up-regulation in pulmonary microvasculature of ventilated preterm infants. Am J Respir Crit Care Med 2008;178:180-187
28. Horie S, Gonzalez HE, Laffey JG, Masterson CH. Cell therapy in acute respiratory distress syndrome. J Thorac Dis 2018;10:5607-5620
29. Huh JW, Kim WY, Park YY, Lim CM, Koh Y, Kim MJ, Hong SB. Anti-inflammatory role of mesenchymal stem cells in an acute lung injury mouse model. Acute Crit Care 2018;33:154-161
30. Gonzales JN, Lucas R, Verin AD. The acute respiratory distress syndrome: mechanisms and perspective therapeutic approaches. Austin J Vasc Med 2015;2:1009
31. Herrero R, Sanchez G, Lorente JA. New insights into the mechanisms of pulmonary edema in acute lung injury. Ann Transl Med 2018;6:32
32. Müller JM, Ziegler-Heitbrock HW, Baeuerle PA. Nuclear factor kappa B, a mediator of lipopolysaccharide effects. Immunobiology 1993;187:233-256
33. Jayasingam SD, Citartan M, Thang TH, Mat Zin AA, Ang KC, Ch'ng ES. Evaluating the polarization of tumor-associated macrophages into M1 and M2 phenotypes in human cancer tissue: technicalities and challenges in routine clinical practice. Front Oncol 2020;9:1512
34. Shin SA, Joo BJ, Lee JS, Ryu G, Han M, Kim WY, Park HH, Lee JH, Lee CS. Phytochemicals as anti-inflammatory agents in animal models of prevalent inflammatory diseases. Molecules 2020;25:5932